

1 *Supplement of*

2 **High-resolution physicochemical dataset of atmospheric aerosols over**
3 **the Tibetan Plateau and its surroundings**

4 **Jianzhong Xu, Xinghua Zhang, et al.**

5 *Correspondence to:* Jianzhong Xu (jz xu78@sjtu.edu.cn; jz xu@lzb.ac.cn); Xinghua
6 Zhang (zhangxinghua@lzb.ac.cn)

7 **Contents of this file**

8 Text S1. HR-ToF-AMS operation

9 Text S2. HR-ToF-AMS data processing

10 Text S3. OA source apportionment using PMF analysis

11 Text S4. Operation and data processing of other instruments

12 1) SMPS; 2) PAX; 3) Aethalometer; 4) CCN-100

13 Text S5. Calculation and evaluation of the bulk acidity of submicron aerosols

14 Text S6. Estimation of aerosol DRFs using the SBDART and OPAC models.

15 **Text S1. HR-ToF-AMS operation**

16 The HR-ToF-AMS is one of the most advanced instruments that widely used for
17 the study of atmospheric aerosol chemistry worldwide. The detailed principle of HR-
18 ToF-AMS can be obtained elsewhere (DeCarlo et al., 2006). The HR-ToF-AMS is
19 mainly composed by three different sections that separated by small apertures and
20 differentially pumped, i.e., a particle beam generation section to form a concentrated
21 and narrow particle beam through a critical orifice and a six-stage aerodynamic lens, a
22 particle-sizing chamber to measure the particle aerodynamic sizes through a particle
23 time-of-flight measurement (different velocities and arrival times for size-dependent
24 particles in a known flight distance), and a particle chemical composition detection
25 section to directly vaporize the particle beam at a ~ 600 °C resistively heated surface,
26 ionize the particles into positively charged ion fragments by a 70 eV electron impact,
27 and then detect their chemical composition by a high-resolution mass spectrometer
28 (Jimenez et al., 2003).

29 There are two different operation modes in HR-ToF-AMS, i.e., V-mode (detection
30 limits of about 10 ng m^{-3}) and W-mode ($\sim 5000 \text{ m}/\Delta\text{m}$) with different signal-to-noise
31 ratio (S/N). However, the HR-ToF-AMSs were only operated at the V-mode during
32 almost all the seven field campaigns in consideration of the relatively low aerosol mass
33 concentration level and low S/N ratio over the TP. The mass concentration and size
34 distribution of non-refractory PM_{10} chemical species were obtained by further switching
35 the instrument between mass spectrum (MS) mode and particle time-of-flight (PToF)
36 mode every 15s under the V-mode operation. However, there are no observation of
37 particle sizes during the NamCo and LHG measurements due to the malfunction of the
38 chopper. In addition, the HR-ToF-AMS need to be calibrated for its flow, ionization
39 efficiency (IE), and sizes at the beginning and end of each observation (Jayne et al.,
40 2000). The relative IE (RIE) of ammonium and sulfate were calibrated using the mono-
41 dispersed pure ammonium nitrate and ammonium sulfate particles, respectively, with
42 the selected sizes of 200–300 nm, while the particle size was calibrated using the mono-
43 dispersed ammonium nitrate particles with sizes varied from 60 to 600 nm. Finally,

44 default RIE values were assumed to be 1.1, 1.3, and 1.4 for nitrate, chloride, and OA,
45 respectively, during all the field campaigns, while different RIE values were set for
46 ammonium and sulfate according to their calibration results during each campaign, e.g.,
47 3.9 and 4.2 for ammonium and 1.6 and 1.4 for sulfate based on two calibrations in the
48 QOMS measurement.

49 **Text S2. HR-ToF-AMS data processing**

50 The HR-ToF-AMS data was processed using the standard data analysis software
51 with SQUIRREL and PIKA toolkits written in Igor Pro (Wavemetrics Inc., Lake
52 Oswego, OR, USA). The SQUIRREL used a fragmentation table to apportion the
53 measured signals at each mass-to-charge ratio (m/z) into different species to quantify
54 the chemical composition of non-refractory PM₁ species, while the PIKA employed a
55 modified Gaussian fitting algorithm to obtain the ion-specified high-resolution mass
56 spectra (HRMS) and elemental composition of OA (Allan et al., 2004; DeCarlo et al.,
57 2006). The elemental ratios of OA, i.e., oxygen-to-carbon (O/C), hydrogen-to-carbon
58 (H/C), organic matter-to-organic carbon (OM/OC), and nitrogen-to-carbon (N/C), were
59 determined using the improved method (Canagaratna et al., 2015) during all the seven
60 observation campaigns.

61 In addition, a collection efficiency (CE) was generally introduced to compensate
62 for the incomplete transmission and detection of particles through the aerodynamic lens
63 and bouncing at the vaporizer surface in most AMS studies. Previous study has revealed
64 that the CE is significantly influenced by the relative humidity (RH) in sampling line
65 and the acidity and ammonium nitrate mass fraction (ANMF) in the sampled aerosols,
66 which has been concluded as a build-in composition-dependent CE (CDCE) algorithm
67 in the standard data processing software (Middlebrook et al., 2012). Generally, a high
68 RH, a high aerosol acidity, or a high ANMF often corresponds to a high CE value.
69 However, the RH in the sampling system is always maintained below 40% due to the
70 professional deployments of dryers in the front of the sampling system and the ANMF
71 is basically below 0.4 due to the low contributions of nitrate and ammonium during all
72 the seven observation campaigns, which means the negligible effects of these two

73 parameters on CE in our study. Therefore, default CE value of 0.5 were finally
74 employed during the QOMS, NamCo, Ngari, Waliguan, and Lhasa campaigns in
75 consideration of their overall neutralized or slightly acidic aerosols, whereas the CDCE
76 values were adopted at Motuo, LHG, and Bayanbulak where bulk submicron aerosols
77 were acidic.

78 **Text S3. OA source apportionment using PMF analysis**

79 Source apportionment of OA during each observation was conducted by the
80 positive matrix factorization (PMF) analysis on organic matrix data using the PMF2.exe
81 algorithm in robust mode (Paatero and Tapper, 1994) and the standard PMF Evaluation
82 Tool (PET, Ulbrich et al., 2009) written in Igor Pro software.

83 The PMF analysis was evaluated thoroughly according to the standard procedures
84 outlined in Zhang et al. (2011) by down-weighting, modifying, or removing some ion
85 fragments in the data and error matrices. Firstly, those ions at $m/z > 120$ and all the
86 isotope ions were generally excluded because of the insufficient ability to resolve the
87 deconvolution due to their low signals. Then, the signals of the four organic ions of O^+ ,
88 HO^+ , H_2O^+ , and CO^+ were scaled to that of CO_2^+ according to the suggested
89 fragmentation table in Aiken et al. (2008) and further down-weighted in PMF analysis.
90 Thirdly, all those “bad” ions ($S/N < 0.2$) were removed from the data matrices, while all
91 the “weak” ions ($0.2 < S/N < 2$) were downweighted by increasing their errors. In
92 addition, some runs and some ions which had obviously huge residual spikes were also
93 removed in order to avoid their unnecessary interference. After the above pre-
94 processing, the PMF solutions were investigated by selecting a certain variation range
95 of factor number and rotational parameter ($fPeak$), e.g., 1–6 factors with $fPeak$ varying
96 from -1 to 1 . Finally, the optimal solution of PMF analysis were determined after a
97 comprehensive evaluation by examining the model residuals at each m/z and each time,
98 comparing the factor mass spectrum with corresponding reference spectrum, comparing
99 the temporal variation of individual factor with external tracers, and analyzing the
100 diurnal variation pattern of each factor. Totally, 2-, 3-, or 4-factor solution were selected
101 during the different field campaigns in this study. The specific high-resolution mass

102 spectrum of each OA factor identified among the eight different field campaigns are
103 shown in Figure S4.

104 **Text S4. Operation and data processing of other instruments**

105 **1) SMPS**

106 The scanning mobility particle sizer (SMPS) developed by the TSI Inc. is
107 composed by an electrostatic classifier (EC, model 3080) equipped with a long-
108 differential mobility analyzer (long-DMA, model 3081) and a condensed particle
109 counter (CPC, model 3772). Ambient particles are first screened by a particle impactor
110 installed at the front of the DMA and large particles are removed. Ambient particles are
111 measured through an electrical mobility detection technique in this instrument, e.g., a
112 bipolar charger in the EC is utilized to charge the particles to a known charge
113 distribution, then classify them according to their ability to traverse an electrical field
114 in the long-DMA, and finally count those screened monodisperse particles by the CPC.
115 The sample and sheath flow rates are 0.3 and 3.0 L min⁻¹, respectively, at both QOMS
116 and Lhasa which measure particles between 14.6 and 661.2 nm in mobility diameter
117 (D_m), whereas the sample and sheath flow rates are 0.5 and 5.0 L min⁻¹ at LHG and
118 Motuo and sample particles at a size range of 10.9–495.8 nm in D_m . The number
119 concentrations of submicron particles in 107 different size channels are firstly recorded
120 at an initial time resolution of 5 min and then converted to the total number and volume
121 concentrations according to the obtained size distribution of number concentration.

122 **2) PAX**

123 The PAX directly measures the B_{abs} and B_{scat} of aerosol particles at 405 nm by
124 using a modulated diode laser, namely measures the B_{abs} by an in-situ photoacoustic
125 technique while the B_{scat} using a wide-angle integrating reciprocal nephelometer. The
126 B_{ext} is the sum of B_{abs} and B_{scat} while the single scattering albedo (SSA) is calculated as
127 the ratio of B_{scat} to B_{ext} . The BC mass concentration is calculated as the ratio of measured
128 B_{abs} to a fixed BC mass absorption cross-section (MAC) value of 10.19 m²g⁻¹ at 405
129 nm. In addition, the B_{scat} is calibrated using the high-concentration ammonium sulfate
130 particles generated by the aerosol generator, while the B_{abs} is calibrated using the

131 sufficient black smoke from a kerosene lamp before each field campaign according to
132 the operator manual of this instrument.

133 **3) Aethalometer**

134 The Aethalometer (models AE31 or AE33) is used to measure the particle B_{abs} at
135 seven wavelengths, which firstly measures the light attenuation between particle-laden
136 and particle-free sample spots on the filter and finally converts the attenuation to
137 particle B_{abs} in ambient air. Both AE31 and AE33 have seven bands, namely 370, 470,
138 520, 590, 660, 880 and 950 nm, and the concentration of black carbon is mainly
139 measured according to the absorption coefficient at 880 nm. The filter-based loading
140 effect and multiple scattering effect are corrected during all the three observations to
141 eliminate the difference between the light attenuation measured at the filter and the
142 ambient particle B_{abs} .

143 The absorption Ångström exponents (AAE) value is acquired through a power-
144 law fitting of B_{abs} following the typical Beer-Lambert's law, i.e., $AAE =$
145 $\ln(B_{abs,\lambda_1}/B_{abs,\lambda_2})/\ln(\lambda_2/\lambda_1)$. Furthermore, a traditional AAE method was adopted to
146 quantitatively apportion the total B_{abs} into two parts from BC and BrC ($B_{abs,BC}$ and
147 $B_{abs,BrC}$) at 370–660 nm during each campaign. The contribution of BrC to total B_{abs}
148 ($fB_{abs,BrC}$) at a short wavelength λ is calculated as $fB_{abs,BrC,\lambda} = 1 - (B_{abs,880}/B_{abs,\lambda}) \times$
149 $(\lambda/880)^{-AAE_{BC}}$ by assuming its negligible contribution at 880 nm. Detailed information
150 about the data correction and calculation of this instrument can be found in our previous
151 publication (Zhang et al., 2021b).

152 **4) CCN-100**

153 The CCN-100 measures aerosol particles called cloud condensation nuclei that can
154 form into cloud droplets. The instrument supersaturates the sampled aerosol particles
155 in a 50-cm-high column with continuously wetted walls and a longitudinal thermal
156 gradient, so that those particles grow into detectable CCN particles and are measured
157 using an optical particle counter among 20 different size bins. The principle of CCN
158 counters is that diffusion of heat in ambient air is slower than that of water vapor, which
159 diffuses from the warm, moist column walls to the centerline faster than heat in the

160 column. Detail information may refer to Roberts and Nenes (2005). The number
161 concentrations of CCN are measured consecutively at five different *SS* values of 0.2%,
162 0.4%, 0.6%, 0.8%, and 1.0%. The CCN data is recorded every 5 minutes at each *SS* and
163 finally has a time resolution of 30 minutes during a complete measurement cycle.

164 **Text S5. Calculation and evaluation of the bulk acidity of submicron aerosols**

165 Bulk acidity of submicron aerosols from AMS measurement was generally
166 evaluated following the methods in Zhang et al. (2007) and Schueneman et al. (2021).
167 The mass concentration of ammonium was firstly predicted by assuming to fully
168 neutralize these AMS measured sulfate, nitrate, and chloride using the following
169 equation:

$$170 \quad \text{NH}_4^+_{\text{Predicted}} = 18 \times (2 \times \text{SO}_4^{2-}/96 + \text{NO}_3^-/62 + \text{Cl}^-/35.5) \quad (1)$$

171 Then, the mass concentration ratio of measured ammonium to predicted
172 ammonium ($\text{NH}_4^+_{\text{Measured}}/\text{NH}_4^+_{\text{Predicted}}$) was further calculated to be a good indicator to
173 evaluate the bulk acidity of submicron aerosols. In this study, linear regression analysis
174 between the mass concentrations of measured and predicted ammonium was performed
175 to evaluate the bulk acidity of submicron aerosols in the different TP regions (Fig. 3).
176 Aerosol particles are generally considered to be “acidic” if the calculated ratio is
177 obviously lower than 1 and to be “more acidic” if the ratio is lower than 0.75, whereas
178 a ratio that roughly near to 1 or larger than 1 indicates the particles are “bulk neutralized”
179 and even there are more excess ammonium that needed to be neutralized. Note that the
180 validity of using this method is based on the assumption that the influence from
181 nitrogen- or sulfur-containing organic ions (e.g., organic acids and organic nitrogen
182 compounds) as well as the mineral and metal ions are negligible (Zhang et al., 2007).

183 **Text S6. Estimation of aerosol DRFs using the SBDART and OPAC models.**

184 The aerosol direct radiative forcing (DRF) was modelled by the widely used Santa
185 Barbara DISORT (Discrete Ordinate Radiative Transfer) Atmospheric Radiative
186 Transfer (SBDART) model in the shortwave spectral range of 0.25–4.0 μm . SBDART
187 is a software tool that computes the plane-parallel radiative transfer under both clear

188 and cloudy conditions (Ricchiazzi et al., 1998). Specific simulation of aerosol DRF in
 189 the atmosphere (ATM) can be described by the following equations (2) and (3). In brief,
 190 the net fluxes (ΔF , difference between the downward and upward radiation fluxes) with
 191 and without the investigated variable were calculated twice in this model under cloud-
 192 free conditions at both the earth's surface (SUR) and the top of the atmosphere (TOA).
 193 The differences of net fluxes between the two simulations were then considered as the
 194 DRFs of the specific investigated variable at the SUR and TOA. Finally, the DRF in
 195 the ATM (DRF^{ATM}) was obtained using the DRF at TOA (DRF^{TOA}) minus the DRF at
 196 SUR (DRF^{SUR}). The details of the model description can be found in previous studies
 197 (Xin et al., 2016; Gong et al., 2017).

$$198 \quad \Delta F = F^{\text{downward}} - F^{\text{upward}} \quad (2)$$

$$199 \quad DRF^{ATM} = DRF^{TOA} - DRF^{SUR} = (\Delta F_{\text{with}}^{TOA} - \Delta F_{\text{without}}^{TOA}) - (\Delta F_{\text{with}}^{SUR} - \Delta F_{\text{without}}^{SUR}) \quad (3)$$

200 The principle and specific steps for the estimation of aerosol DRFs using the
 201 SBDART mode can be described briefly as follows:

202 Firstly, the mass concentrations of organic carbon (OC), BC, and water-soluble
 203 ions (WSIs), which were measured from the corresponding off-line filter samples with
 204 one- or two-days time resolutions during each campaign, were the initial measured
 205 parameters used for the estimation of aerosol DRFs.

206 Then, the particle numbers of each species in per cubic meter air (denoted as ρ_n)
 207 were estimated using the above measured mass concentrations of each species divided
 208 by the referred M values in the OPAC model (Hess et al., 1998), which represented the
 209 aerosol mass in per cubic meter air and integrated over the size distribution and
 210 normalized to 1 particle per cubic centimeter of air. Specifically, values of 5.99E-5 was
 211 used for soot/BC particles and 1.34E-3 were used for OC and WSIs.

212 Next, four crucial input optical parameters of aerosol optical depth (AOD), single
 213 scattering albedo (SSA), Ångström exponent (AE), and asymmetry factor (ASY), and
 214 the light absorption and scattering coefficients were estimated for OC, BC, WSIs and
 215 total particles, respectively, using the Optical Properties of Aerosol and Cloud (OPAC)

216 model. Detailed introduction of OPAC model can be found in Hess et al. (1998). Noting
217 that the above estimation in OPAC model were performed six times during each
218 campaign by setting the ρ_n as the above calculated value multiplier 1 to 6, respectively.

219 Then, the entire six datasets of modelled total light absorption and scattering
220 coefficients were further used to evaluate the performance of OPAC model by
221 comparing them with those corresponding measured light absorption and scattering
222 coefficients from PAX and Aethalometer (Figures S6-10). Finally, the optimal ρ_n
223 value was selected when the modelled total light absorption and scattering coefficients
224 were comparable.

225 The performance of the OPAC model was then evaluated and tuned by comparing
226 the modelled total light scattering and absorption coefficients with those
227 correspondingly measured values from online Aethalometer and PAX measurements
228 during the three campaigns, as shown in Figures S5-10. The consistent variation trends
229 were found between them with the coefficient of determination (R^2) varying between
230 0.69 and 0.99. The slightly lower modelled values compared with those measured
231 values was mainly attributed to their inconsistent wavelengths, i.e., the modelled light
232 scattering and absorption coefficient at 550 nm in the OPAC model, whereas the
233 measured light scattering coefficients at 405 nm for PAX and the light absorption
234 coefficients at 520 nm for Aethalometer. Overall, the small difference between the
235 modelled and measured values indicated the reasonable simulation of aerosol optical
236 parameters (e.g., AOD, AE, SSA, and ASY) in the OPAC model in this study. Finally,
237 these four optical parameters belonging to each species were all used in the SBDART
238 model for the simulation of DRFs caused by OC, BC, and WSIs.

239 After the above evaluation, the finally obtained four input parameters of AOD,
240 SSA, AE and ASY belong to each species (OC, BC, WSIs, and total particles) were
241 inputted into the SBDART model to simulation the DRFs of each species, respectively.

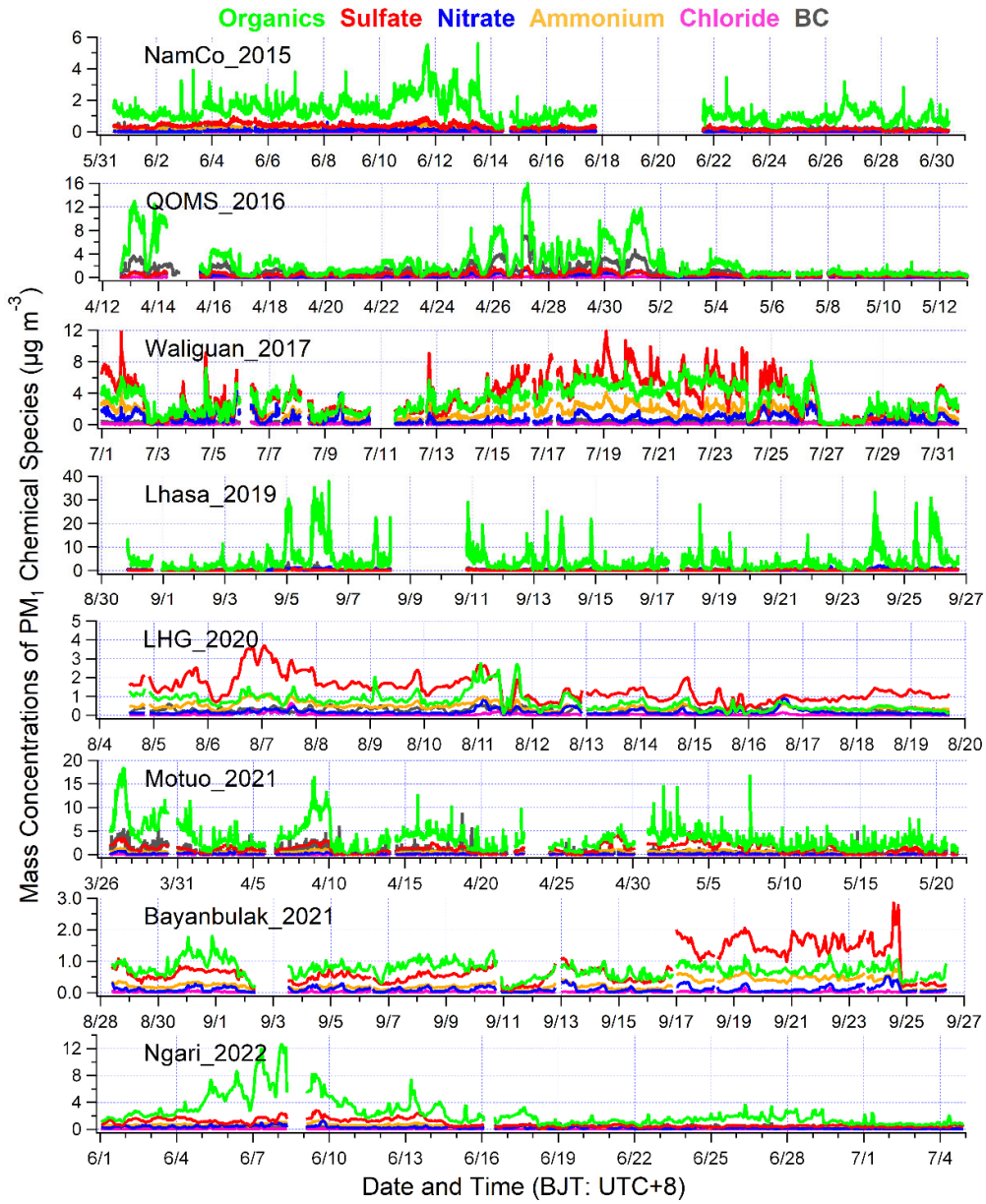
242 **Table S1. Summary of measurements on ambient aerosols in the TP by different off-line filter sampling and on-line instruments.**

	Measurement content	Period	Site	Instrument/Method	Resolutions	References	
	Off-line filter sample analysis for aerosol concentration and chemical composition: CAs (BC/EC/OC/WSOC/BrC), WSIs, element, etc.						
1.	BC and OC dataset over the Third Pole	Different periods during different campaigns	19 stations from APCC network	TSP samples	off-line, 24-48 h	Kang et al. (2022)	
2.	CAs characteristics on the Third Pole			TSP samples	off-line, 24-48 h	Chen et al. (2019a)	
3.	CAs in the TP: An investigative review			Lhasa, Lulang, Nam Co, QOMS, etc.	PM _{2.5} and TSP samples	off-line	Li et al. (2021a)
4.	BC sources reaching the TP			7 stations across the Himalayas	TSP samples	off-line, 24-48 h	Li et al. (2016a)
5.	Concentrations and light absorption of CAs	2013/5-2014/3	Lhasa, urban city	PM ₁₀ and PM _{2.5} samples	off-line, 12-24h/week	Li et al. (2016b)	
6.	CAs (OC and BC)	2006/7-2009/12	Nam Co, inland TP	TSP samples	off-line, 4-14 days	Zhao et al. (2013a)	
7.	Mass, elements, CAs, and WSIs	2008/7/16-2009/7/26	Lulang, southeastern TP	TSP samples	off-line, 6 days	Zhao et al. (2013b)	
8.	Concentrations, seasonality and sources of CAs	2009/8-2010/7	QOMS, southern TP	TSP samples	off-line, 24 h/week	Cong et al. (2015)	
9.	Size distribution of CAs	2012	Nam Co, inland TP	Size-segregated samples	off-line, 72 h	Wan et al. (2015)	
10.	Size-segregated characteristics of CAs	2014/8-9,11-12	Lhasa, urban city	Six-stage cascade impactors	off-line	Wei et al. (2019a)	
11.	Near surface PM _{2.5} concentration	2016/12/20-12/26	Lhasa, urban city	PM _{2.5} samples	off-line, 12 h	Li et al. (2019)	
12.	BC concentrations	2003/12/5-2006/2/17	Muztagh Ata Mountain, northern TP	TSP samples	off-line, 1 week	Zhou et al. (2018)	
13.	Elemental concentrations	2005/11-2007/11	Nam Co Station, inland TP	TSP samples	off-line, weekly	Kang et al. (2016)	
14.	Elemental composition	2019/12-2020/11	Yaze, southeastern TP	TSP samples	off-line, 15 days	Xu et al. (2022b)	
15.	Elements and WSIs	2009/3-5,7-8,11-12	Lijiang, southeastern TP	TSP samples	off-line, 1-2 days	Zhang et al. (2016)	
16.	Characteristics of WSIs	2010/7/16-2011/7/28	Qilian Shan, northeastern TP	PM _{2.5} samples	off-line, weekly	Xu et al. (2014)	
17.	Seasonal variations and size distributions of WSIs	2012/10-2013/9	Shigatse, southern TP	Eight-stage impactor	off-line, weekly	Yang et al. (2016)	
18.	Characteristics of size distributions and sources of WSIs	2014/8-9,11-12	Lhasa, urban city	Six-stage cascade impactors	off-line	Wei et al. (2019b)	
19.	OC, EC, WSOC and HULIS	2014/12/21-2015/2/2 2015/8/3-9/7	Nam Co, inland TP	TSP samples	off-line, 12 h	Wu et al. (2018)	
20.	Overestimation of BC concentration caused by high OC	2018/7-2019/7; 2020/4- 2021/3; 2017/1-2017/12	Yaze, southeastern TP;; QOMS, southern TP; Nam Co, inland TP	TSP samples	off-line, 2-20 days	Hu et al. (2023)	
21.	Chemical composition of PM _{2.5} and TSP	2010/6-2010/9	Qinghai Lake, northeastern TP	PM _{2.5} and TSP samples	off-line, 3 days	Zhang et al. (2014)	
22.	Chemical characterization and sources of PM _{2.5}	2015/5-2016/5	Mt. Gongga, eastern TP	PM _{2.5} samples	off-line, weekly	Meng et al. (2020)	
23.	Chemical composition and size distribution of PM _{2.5}	2012/7/11-9/6	Qilian Shan, northeastern TP	PM _{2.5} samples	off-line, 3 days	Xu et al. (2015)	
24.	Chemical compositions in PM _{2.1}	2012/4-2014/12	Mt. Gongga, eastern TP	Nine-stage Anderson sampler	off-line, 48 h	Su et al. (2018)	
25.	Chemical composition of size-segregated aerosols	2013/3-2014/2	Lhasa, urban city	Size-segregated samples	off-line, 2 weeks	Wan et al. (2016)	
26.	Chemical composition and optical properties	2016/4/12-5/12	QOMS, southern TP	PM _{2.5} samples	off-line, 48 h	Xu et al. (2020)	
27.	Molecular composition and optical properties of WS-BrC	2017/7/1-7/31	Waliguan, northeastern TP			Xu et al. (2022a)	
28.	Characteristics and sources of PM _{2.5}	2018/3/11-5/13	Gaomeigu, southeastern TP	PM _{2.5} samples	off-line, 24 h	Zhao et al. (2019b)	
29.	Abundance, composition and source of PM _{2.5}	2010/7/3-8/26	Qinghai Lake, northeastern TP	PM _{2.5} samples	off-line, 24 h	Li et al. (2013)	
30.	Seasonal/diurnal variation of molecular tracers for OAs	2014/12/21-2015/2/1 2015/8/4-9/6	Nam Co, inland TP	TSP samples	off-line, 12 h	Wan et al. (2023)	

Off-line filter sample analysis for aerosol light absorption of CAs (BC/EC/OC/WSOC/BrC/HULIS)						
31.	Light absorption of CAs	2014/8-2015/8	QOMS and Lulang	TSP samples	off-line, 2 samples/month	Li et al. (2016c)
32.	Seasonal variation and light absorption property of CAs	2014/12-2016/12	Mt. Yulong and Ganhaizi basin	TSP samples	off-line, 6 days	Niu et al. (2017)
33.	Light absorption by WSOC	2015/6/2-7/1	Nam Co Station, inland TP	PM _{2.5} samples	off-line, 24 h	Zhang et al. (2017)
34.	Sources and light absorption characteristics of WSOC	2016/11-2017/11	Nam Co, inland TP	PM _{2.5} and TSP samples	off-line	Li et al. (2021b)
35.	Multi-wavelength light absorption of BC and BrC	2008/7/16-2009/7/26	Lulang, southeastern TP	TSP samples	off-line, 72 h	Zhao et al. (2019a)
36.	Light absorption, fluorescence properties and sources of BrC	2013/8-2014/1	Lulang, southeastern TP	TSP samples	off-line, 11.5 h	Wu et al. (2020)
37.	Light absorption properties of BrC	2015/11-2016/11	Lulang, southeastern TP	TSP samples	off-line, weekly	Zhu et al. (2018)
38.	Light absorption of CAs from the Sichuan Basin to TP	2018/12/21-2019/12/18	Six sites from SCB to TP	PM ₁ samples	off-line, day/night	Zhao et al. (2022a)
39.	Molecular compositions and light absorption of HULIS	2015/3/22-2015/4/14	Mt. Yulong, southeastern TP	PM _{2.5} samples	off-line, 48 h	Wang et al. (2019b)
Off-line filter sample analysis for PAHs, Individual particle analysis by TEM, Isotope Analysis, and others						
40.	Concentrations of PAHs	2008/8/5-2009/7/13	Lhasa, urban city	TSP samples	off-line, 24 h/week	Ma et al. (2013)
41.	Source apportionment and risk assessment of atmospheric PAH	2013/4-2014/3	Lhasa, urban city	TSP samples	off-line, 24 h	Chen et al. (2018a)
42.	n-Alkanes and PAHs	2015/11-2016/11	Lulang, southeastern TP	TSP samples	off-line, weekly	Zhu et al. (2020)
43.	Individual particle analysis (Mixing state and sources)	2013/9/15-10/15	Menyuan, northeastern TP	TEM samples	off-line	Li et al. (2015)
44.	Individual particle analysis (Mixing State and Fractal Dimension)	2016/5/26-6/2	Lulang, southeastern TP	TEM samples	off-line	Yuan et al. (2019)
45.	Individual particle analysis (composition and sources)	2013/2/2-3/8	Lhasa, urban city	TEM samples	off-line	Duo et al. (2015)
46.	Radiocarbon and stable isotope ¹³ C of OC and EC	2018/9-2019/8	Qinghai Lake, northeastern TP	TSP samples	off-line, 1 week	Ni et al. (2023)
47.	Δ ¹⁴ C and δ ¹³ C of TC and IPC	2020/7-2021/6	Hongyuan, eastern TP	PM _{2.5} and TSP samples	off-line, every 2 weeks	Li et al. (2022)
48.	Stable isotope (¹⁵ N) analysis of nitrogen compounds	2017/3/23-2018/3/19	QOMS, southern TP	TSP samples	off-line	Bhattarai et al. (2023)
49.	Nitrogen and oxygen isotopic compositions	2017/3-2018/2	QOMS, southern TP	TSP samples	off-line, 1 week	Lin et al. (2021)
50.	S-isotope characteristic	2021/3-2021/6	QOMS, southern TP	PM _{2.5} samples	off-line, 96 h	Dasari et al. (2023)
51.	Primary biological aerosol particles (PBAPs)	2018/8-2019/9; 2018/9-2019/7; 2019/7-2020/7	Qinghai lake, Beiluhe, Ngari	TSP samples	off-line	Zhu et al. (2022)
52.	Oxalic acid and related SOA	2010/7-2010/8	Qinghai Lake, northeastern TP	PM _{2.5} samples	off-line, 24 h	Meng et al. (2013)
On-line measurement of BC concentration and light absorption of BC and BrC by Aethalometers and other optical instruments						
53.	Concentration, temporal variation, and sources of BC	2015/5/15-2017/5/31	QOMS, southern TP	AE-33 Aethalometer	on-line, 1-min	Chen et al. (2018b)
54.	BC concentration	2009/5-2011/3	Qilian Shan, northeastern TP	AE-31 Aethalometer	on-line, 5-min	Zhao et al. (2012)
55.	BC concentration	2008/11-2009/1	Linzi, southeastern TP	AE-16 Aethalometer	on-line, 5-min	Cao et al. (2011)
56.	Aerosol light absorption	Autumn 2015	Lhasa and Lulang	AE-33 Aethalometer	on-line, 1-min	Zhu et al. (2017)
57.	Light absorption contributions of BC, BrC _{pri} , and BrC _{sec}	2018/8-2019/9; 2018/9-2019/7; 2019/7-2020/7	Qinghai lake, Beiluhe, Ngari	AE-33 Aethalometer	on-line	Zhu et al. (2021)
58.	Secondary BrC absorption	2018/3/14-5/13	Gaomeigu, southeastern TP	AE-33 Aethalometer	on-line, 1-min	Wang et al. (2019a)
59.	Source contribution of fossil fuels and biomass-burning BC	2018/3/14-5/13	Lijiang, southeastern TP	AE33 Aethalometer/PAX	on-line	Liu et al. (2021)
60.	Mass concentrations, size distributions, mixing states, and light absorption properties of refractory BC	2015/9/17-10/31	Lulang, southeastern TP	SP2 and PAX	on-line, hourly	Wang et al. (2018)

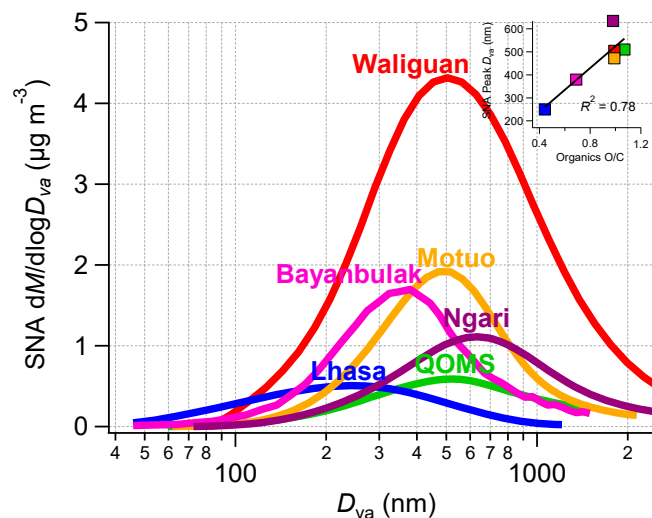
61.	Light absorption properties of BC and BrC	2015/5/31-7/1 2016/4/12-5/12 2017/7/1-7/31	Nam Co, inland TP QOMS, southern TP Waliguan, northeastern TP	Aethalometer PAX/MAAP HR-ToF-AMS	on-line, 5-min on-line, hourly	Zhang et al. (2021b)
62.	Optical properties, size distributions, chemical compositions	2019/7/8-8/2	Shiquanhe, southwestern TP	Nephelometer/PAX/APS	on-line, 10s-5 min	Zhang et al. (2021a)
63.	Optical characteristics of aerosol	2020/8/5-9/11	Nam Co, inland TP	APS/MAPP	on-line, 5/1-min	Wang et al. (2023)
On-line measurement of aerosol mass and number concentrations by TEOM RP1400, SMPS, and other instruments						
64.	Concentrations of BC, PM _{2.5} , PM ₁₀ , and CAs and WSIs	2004/4/7-5/24	Tengchong, southeastern TP	TEOM RP1400/Aethalometer PM _{2.5} and PM ₁₀ samples	on-line, 5-min off-line, 24-48 h	Engling et al. (2011)
65.	Characteristics of aerosol mass loadings	2011–2013	Ngari, QOMS, Nam Co, SET	TEOM RP1400 PM _{2.5} samples	on-line, 5-min off-line, 3 days	Liu et al. (2017)
66.	Spatial and temporal variations of particulate pollutants	2016/6-2017/5	Lhasa, Ngari, Qamdo, Nyingchi, Nagchu, and Shigatse	CNEMC download data	on-line, hourly	Chen et al. (2019b)
67.	New particle formation	2019/4/26-5/22 2019/6/15-6/25	Nam Co, inland TP	SMPSs AE-33 Aethalometer	on-line	Tang et al. (2022)
68.	Vertical profiling of particle size distributions	2020/8/8-8/28	Lhasa, urban city	POPS and GRIMM 11-C attached to a tethered balloon	on-line	Ran et al. (2022)
69.	Aerosol number size distribution	2016/8/2-8/20	Lhasa, urban city	Optical particle size spectrometer	on-line, 10-min	Cui et al. (2018)
70.	First simultaneous measurements of PAN and O ₃	summer in 2011/2012	Nam Co, inland TP	PAN Analyzer	on-line, 10-min	Xu et al. (2018b)
71.	Measurements of O ₃ and PAN as well as their precursors	2019/5/1-7/31	Nam Co, inland TP	GC-ECD analyzer	on-line	Xu et al. (2023)
On-line measurement of ambient aerosol chemical composition by aerosol mass spectrometers						
72.	Chemical characterization of PM ₁	2013/9/5-10/15	Menyuan, northeastern TP	ACSM	on-line, 15-min	Du et al. (2015)
73.	Chemical composition of PM ₁	2015/3/22-4/14	Mt. Yulong, southeastern TP	HR-ToF-AMS	on-line, 5-min	Zheng et al. (2017)
74.	Chemical characterization of rBC	2015/5/30-6/30	Nam Co, inland TP	SP-AMS/HR-ToF-AMS MAAP	on-line, 5-min	Wang et al. (2017)
75.	Chemical characteristics and sources of PM ₁	2015/5/31-7/1	Nam Co, inland TP	HR-ToF-AMS/SMPS/MAAP etc.	on-line, 5-min	Xu et al. (2018a)
76.	Chemical characteristics and sources of PM ₁	2016/4/12-5/12	QOMS, southern TP	HR-ToF-AMS/SMPS/PAX	on-line, 5-min	Zhang et al. (2018)
77.	Chemical characteristics and sources of PM ₁	2017/7/1-7/31	Waliguan, northeastern TP	HR-ToF-AMS/PAX/CCN-100	on-line, 10-min	Zhang et al. (2019)
78.	Chemical characteristics and sources of PM ₁ during a festival	2017/7/5-7/6	Waliguan, northeastern TP	HR-ToF-AMS/PAX/CCN-100	on-line, 10-min	Zhang et al. (2020)
79.	Chemical characteristics and sources of PM ₁	2019/8/31-9/26	Lhasa, urban city	HR-ToF-AMS/SMPS/PAX	on-line, 5-min	Zhao et al. (2022b)
80.	Regional difference of aerosol chemical compositions and sources in the TP and its surroundings	Different periods during 2015-2022	QOMS, Motuo, NamCo, Ngari, Waliguan, LHG, Bayanbulak, and Lhasa	HR-ToF-AMS SMPS/ /CCN-100 PAX/Aethalometer	on-line, hourly	This study

243 **Abbreviation:** BC: black carbon; OC: organic carbon; EC: elemental carbon; CAs: carbonaceous aerosols; WSOC: water soluble organic carbon; BrC: brown carbon; WSIs:
244 water soluble ionic species; HULIS: Humic-Like Substances; SOA: secondary organic aerosol; TEM: Transmission electron microscopy; TC: total carbon; IPC: water-insoluble
245 particulate carbon; PAH: polycyclic aromatic hydrocarbons; PAN: peroxyacetyl nitrate; APCC: Atmospheric Pollution and Cryospheric Change; CNEMC: China National
246 Environmental Monitoring Center;



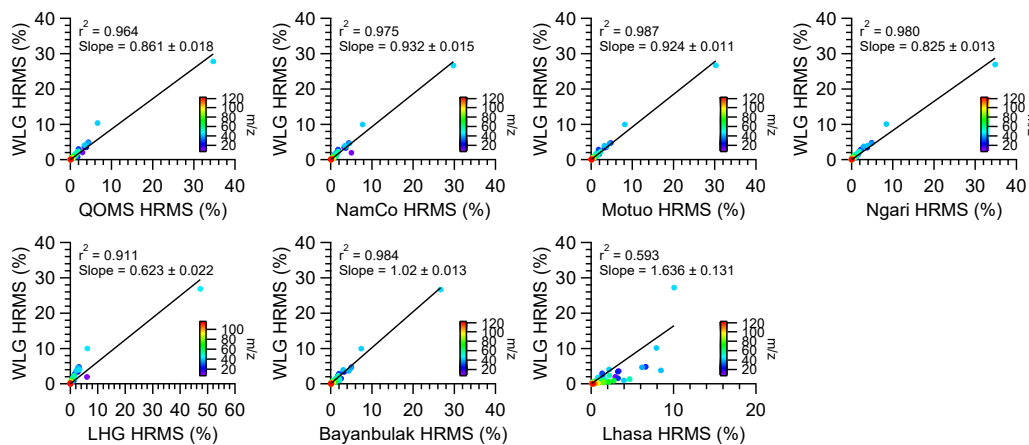
248

249 **Figure S1.** High-time-resolution temporal variations of the mass concentrations of PM₁ chemical
 250 compositions during the eight online aerosol field measurement campaigns over the Tibetan Plateau
 251 and its surroundings.



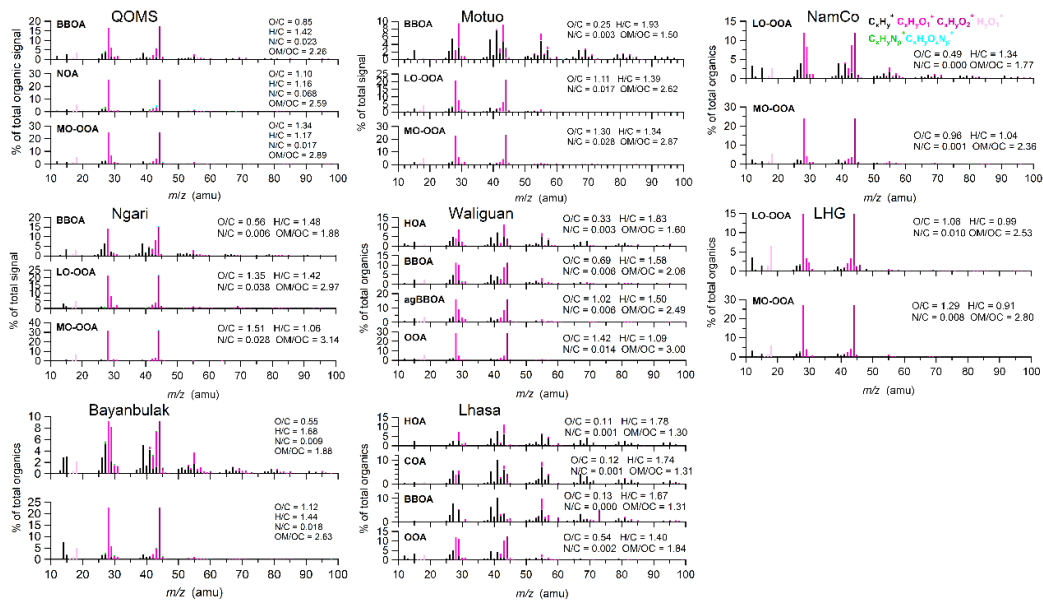
252

253 **Figure S2.** Average size distributions of SNA mass concentrations during six field measurement
 254 campaigns in the Tibetan Plateau and its surroundings. Insert graph is the scatter plot of peak
 255 diameters in these size distributions versus the average O/C ratio of organics.



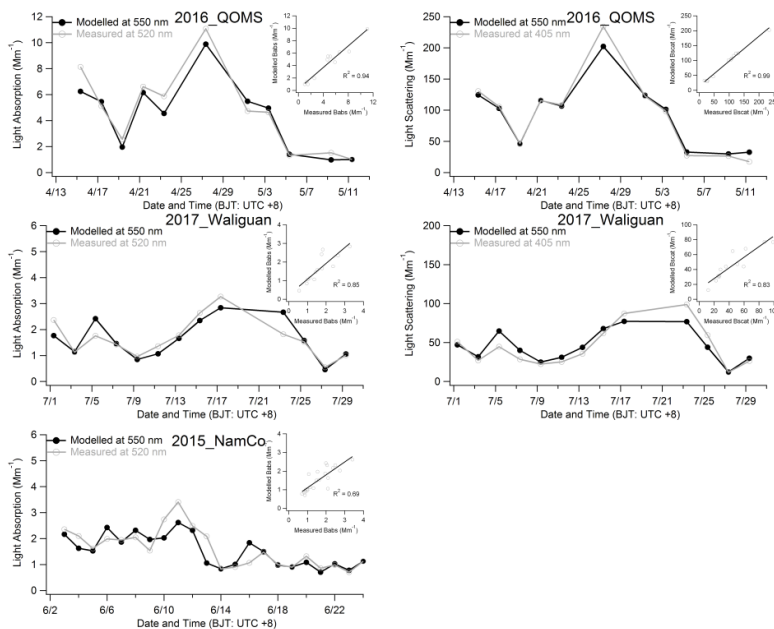
256

257 **Figure S3.** Comparison of OA HRMS between Waliguan and the other seven sites in this study.



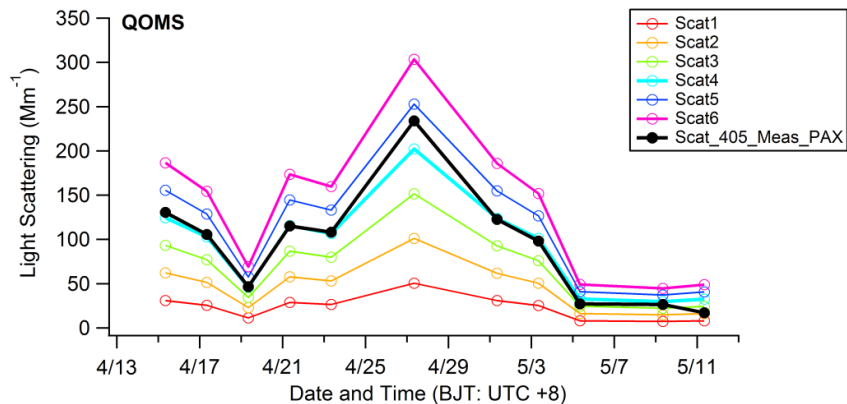
258

259 **Figure S4.** The high-resolution mass spectra (HRMS) of different OA factors identified by the PMF
 260 source apportionment among the eight field campaigns in our study. All the HRMSs are colored by
 261 six ion categories at $m/z < 120$.



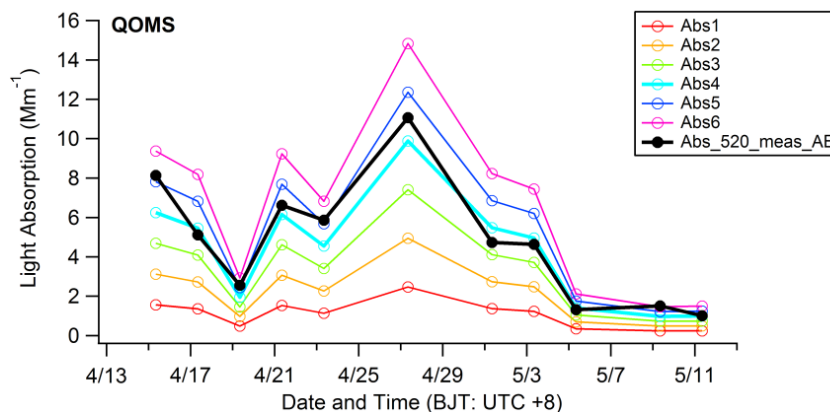
262

263 **Figure S5.** Comparisons of the particle light scattering and absorption coefficients between the
 264 modelled values (final selected) from Optical Properties of Aerosol and Cloud (OPAC) model and
 265 measured values from the photoacoustic extinctions and aethalometer during the three
 266 campaigns.



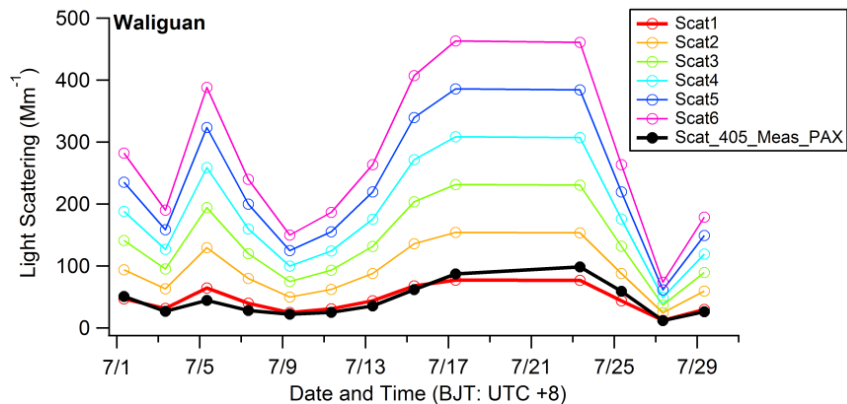
267

268 **Figure S6.** Time series of the particle light scattering coefficients at 405 nm measured by the PAX
 269 and those modelled light scattering coefficients at 550 nm under different particle numbers in per
 270 cubic meter air (the calculated value multiplier 1 to 6, respectively) from the OPAC model during
 271 the QOMS campaign.



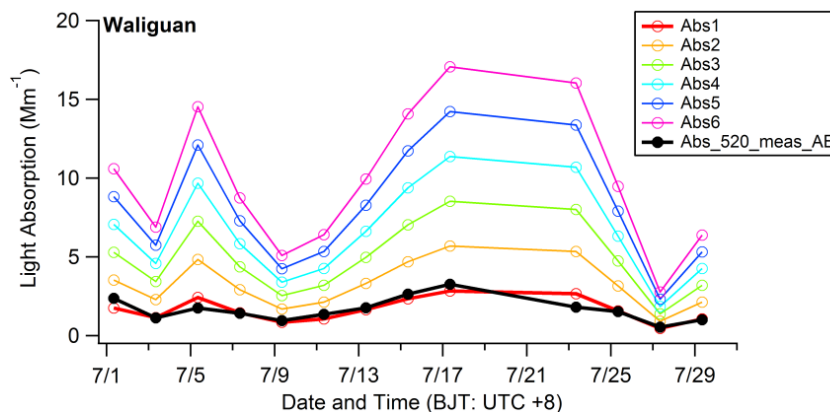
272

273 **Figure S7.** Time series of the particle light absorption coefficients at 520 nm measured by the
 274 Aethalometer and those modelled light absorption coefficients at 550 nm under different particle
 275 numbers in per cubic meter air (the calculated value multiplier 1 to 6, respectively) from the OPAC
 276 model during the QOMS campaign.



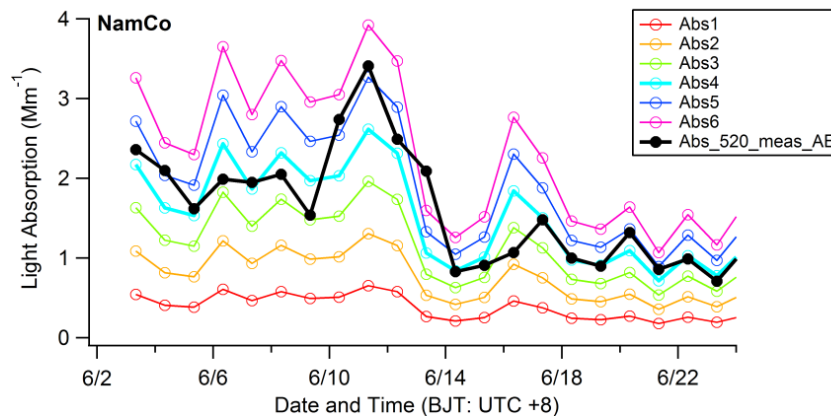
277

278 **Figure S8.** Time series of the particle light scattering coefficients at 405 nm measured by the PAX
 279 and those modelled light scattering coefficients at 550 nm under different particle numbers in per
 280 cubic meter air (the calculated value multiplier 1 to 6, respectively) from the OPAC model during
 281 the Waliguan campaign.



282

283 **Figure S9.** Time series of the particle light absorption coefficients at 520 nm measured by the
 284 Aethalometer and those modelled light absorption coefficients at 550 nm under different particle
 285 numbers in per cubic meter air (the calculated value multiplier 1 to 6, respectively) from the OPAC
 286 model during the Waliguan campaign.



287

288 **Figure S10.** Time series of the particle light absorption coefficients at 520 nm measured by the
 289 Aethalometer and those modelled light absorption coefficients at 550 nm under different particle
 290 numbers in per cubic meter air (the calculated value multiplier 1 to 6, respectively) from the OPAC
 291 model during the NamCo campaign.

References

- Aiken, A. C., DeCarlo, P. F., Kroll, J. H., Worsnop, D. R., Huffman, J. A., Docherty, K. S., Ulbrich, I. M., Mohr, C., Kimmel, J. R., Sueper, D., Sun, Y., Zhang, Q., Trimborn, A., Northway, M., Ziemann, P. J., Canagaratna, M. R., Onasch, T. B., Alfarra, M. R., Prevot, A. S. H., Dommen, J., Duplissy, J., Metzger, A., Baltensperger, U., and Jimenez, J. L.: O/C and OM/OC ratios of primary, secondary, and ambient organic aerosols with high-resolution time-of-flight aerosol mass spectrometry, *Environ. Sci. Technol.*, 42, 4478-4485, 10.1021/es703009q, 2008.
- Allan, J. D., Delia, A. E., Coe, H., Bower, K. N., Alfarra, M. R., Jimenez, J. L., Middlebrook, A. M., Drewnick, F., Onasch, T. B., Canagaratna, M. R., Jayne, J. T., and Worsnop, D. R.: A generalised method for the extraction of chemically resolved mass spectra from Aerodyne aerosol mass spectrometer data, *J. Aerosol Sci.*, 35, 909-922, 10.1016/j.jaerosci.2004.02.007, 2004.
- Bhattacharai, H., Wu, G., Zheng, X., Zhu, H., Gao, S., Zhang, Y. L., Widory, D., Ram, K., Chen, X., Wan, X., Pei, Q., Pan, Y., Kang, S., and Cong, Z.: Wildfire-Derived Nitrogen Aerosols Threaten the Fragile Ecosystem in Himalayas and Tibetan Plateau, *Environ Sci Technol*, 10.1021/acs.est.3c01541, 2023.
- Canagaratna, M. R., Jimenez, J. L., Kroll, J. H., Chen, Q., Kessler, S. H., Massoli, P., Hildebrandt Ruiz, L., Fortner, E., Williams, L. R., Wilson, K. R., Surratt, J. D., Donahue, N. M., Jayne, J. T., and Worsnop, D. R.: Elemental ratio measurements of organic compounds using aerosol mass spectrometry: characterization, improved calibration, and implications, *Atmos. Chem. Phys.*, 15, 253-272, 10.5194/acp-15-253-2015, 2015.
- Cao, J., Tie, X., Xu, B., Zhao, Z., Zhu, C., Li, G., and Liu, S.: Measuring and modeling black carbon (BC) contamination in the SE Tibetan Plateau, *J. Atmos. Chem.*, 67, 45-60, 10.1007/s10874-011-9202-5, 2011.
- Chen, P., Kang, S., Li, C., Li, Q., Yan, F., Guo, J., Ji, Z., Zhang, Q., Hu, Z., Tripathee, L., and Sillanpää, M.: Source Apportionment and Risk Assessment of Atmospheric Polycyclic Aromatic Hydrocarbons in Lhasa, Tibet, China, *Aerosol Air Qual. Res.*, 18, 1294-1304, 10.4209/aaqr.2017.12.0603, 2018a.
- Chen, P., Kang, S., Li, C., Zhang, Q., Guo, J., Tripathee, L., Zhang, Y., Li, G., Gul, C., Cong, Z., Wan, X., Niu, H., Panday, A. K., Rupakheti, M., and Ji, Z.: Carbonaceous aerosol characteristics on the Third Pole: A primary study based on the Atmospheric Pollution and Cryospheric Change (APCC) network, *Environ. Pollut.*, 253, 49-60, 10.1016/j.envpol.2019.06.112, 2019a.
- Chen, P., Yang, J., Pu, T., Li, C., Guo, J., Tripathee, L., and Kang, S.: Spatial and Temporal Variations of Gaseous and Particulate Pollutants in Six Sites in Tibet, China, during 2016–2017, *Aerosol Air Qual. Res.*, 19, 516-527, 10.4209/aaqr.2018.10.0360, 2019b.
- Chen, X., Kang, S., Cong, Z., Yang, J., and Ma, Y.: Concentration, temporal variation, and sources of black carbon in the Mt. Everest region retrieved by real-time observation and simulation, *Atmos. Chem. Phys.*, 18, 12859-12875, 10.5194/acp-18-12859-2018, 2018b.
- Cong, Z., Kang, S., Kawamura, K., Liu, B., Wan, X., Wang, Z., Gao, S., and Fu, P.: Carbonaceous aerosols on the south edge of the Tibetan Plateau: concentrations, seasonality and sources, *Atmos. Chem. Phys.*, 15, 1573-1584, 10.5194/acp-15-1573-2015, 2015.
- Cui, Y. Y., Liu, S., Bai, Z., Bian, J., Li, D., Fan, K., McKeen, S. A., Watts, L. A., Ciciora, S. J., and Gao, R.-S.: Religious burning as a potential major source of atmospheric fine aerosols in summertime Lhasa on the Tibetan Plateau, *Atmos. Environ.*, 181, 186-191, 10.1016/j.atmosenv.2018.03.025, 2018.
- Dasari, S., Paris, G., Pei, Q., Cong, Z., and Widory, D.: Tracing the origin of elevated springtime atmospheric sulfate on the Southern Himalayan-Tibetan Plateau, *Environmental Science: Advances*,

- 10.1039/d3va00085k, 2023.
- DeCarlo, P. F., Kimmel, J. R., Trimborn, A., Northway, M. J., Jayne, J. T., Aiken, A. C., Gonin, M., Fuhrer, K., Horvath, T., Docherty, K. S., Worsnop, D. R., and Jimenez, J. L.: Field-Deployable, High-Resolution, Time-of-Flight Aerosol Mass Spectrometer, *Anal. Chem.*, 78, 8281-8289, 10.1021/ac061249n, 2006.
- Du, W., Sun, Y. L., Xu, Y. S., Jiang, Q., Wang, Q. Q., Yang, W., Wang, F., Bai, Z. P., Zhao, X. D., and Yang, Y. C.: Chemical characterization of submicron aerosol and particle growth events at a national background site (3295 m a.s.l.) on the Tibetan Plateau, *Atmos. Chem. Phys.*, 15, 10811-10824, 10.5194/acp-15-10811-2015, 2015.
- Duo, B., Zhang, Y., Kong, L., Fu, H., Hu, Y., Chen, J., Li, L., and Qiong, A.: Individual particle analysis of aerosols collected at Lhasa City in the Tibetan Plateau, *J Environ Sci (China)*, 29, 165-177, 10.1016/j.jes.2014.07.032, 2015.
- Engling, G., Zhang, Y. N., Chan, C. Y., Sang, X. F., Lin, M., Ho, K. F., Li, Y. S., Lin, C. Y., and Lee, J. J.: Characterization and sources of aerosol particles over the southeastern Tibetan Plateau during the Southeast Asia biomass-burning season, *Tellus B: Chemical and Physical Meteorology*, 63, 117-128, 10.1111/j.1600-0889.2010.00512.x, 2011.
- Gong, C., Xin, J., Wang, S., Wang, Y., and Zhang, T.: Anthropogenic aerosol optical and radiative properties in the typical urban/suburban regions in China, *Atmos. Res.*, 197, 177-187, 10.1016/j.atmosres.2017.07.002, 2017.
- Hess, M., Koepke, P., and Schult, I.: Optical Properties of Aerosols and Clouds: The Software Package OPAC, *Bull. Am. Meteorol. Soc.*, 79, 831-844, 10.1175/1520-0477(1998)079<0831:OPOAAC>2.0.CO;2, 1998.
- Hu, Z., Kang, S., Xu, J., Zhang, C., Li, X., Yan, F., Zhang, Y., Chen, P., and Li, C.: Significant overestimation of black carbon concentration caused by high organic carbon in aerosols of the Tibetan Plateau, *Atmos. Environ.*, 294, 10.1016/j.atmosenv.2022.119486, 2023.
- Jayne, J. T., Leard, D. C., Zhang, X. F., Davidovits, P., Smith, K. A., Kolb, C. E., and Worsnop, D. R.: Development of an aerosol mass spectrometer for size and composition analysis of submicron particles, *Aerosol Sci. Technol.*, 33, 49-70, 10.1080/027868200410840, 2000.
- Jimenez, J. L., Jayne, J. T., Shi, Q., Kolb, C. E., Worsnop, D. R., Yourshaw, I., Seinfeld, J. H., Flagan, R. C., Zhang, X., Smith, K. A., Morris, J. W., and Davidovits, P.: Ambient aerosol sampling using the Aerodyne Aerosol Mass Spectrometer, *J. Geophys. Res.*, 108, 8425, 10.1029/2001jd001213, 2003.
- Kang, S., Chen, P., Li, C., Liu, B., and Cong, Z.: Atmospheric Aerosol Elements over the Inland Tibetan Plateau: Concentration, Seasonality, and Transport, *Aerosol Air Qual. Res.*, 16, 789-800, 10.4209/aaqr.2015.05.0307, 2016.
- Kang, S., Zhang, Y., Chen, P., Guo, J., Zhang, Q., Cong, Z., Kaspari, S., Tripathee, L., Gao, T., Niu, H., Zhong, X., Chen, X., Hu, Z., Li, X., Li, Y., Neupane, B., Yan, F., Rupakheti, D., Gul, C., Zhang, W., Wu, G., Yang, L., Wang, Z., and Li, C.: Black carbon and organic carbon dataset over the Third Pole, *Earth System Science Data*, 14, 683-707, 10.5194/essd-14-683-2022, 2022.
- Li, C., Bosch, C., Kang, S., Andersson, A., Chen, P., Zhang, Q., Cong, Z., Chen, B., Qin, D., and Gustafsson, O.: Sources of black carbon to the Himalayan-Tibetan Plateau glaciers, *Nat. Commun.*, 7, 12574, 10.1038/ncomms12574, 2016a.
- Li, C., Chen, P., Kang, S., Yan, F., Hu, Z., Qu, B., and Sillanpää, M.: Concentrations and light absorption characteristics of carbonaceous aerosol in PM_{2.5} and PM₁₀ of Lhasa city, the Tibetan Plateau, *Atmos. Environ.*, 127, 340-346, <https://doi.org/10.1016/j.atmosenv.2015.12.059>, 2016b.

- Li, C., Yan, F., Kang, S., Chen, P., Hu, Z., Gao, S., Qu, B., and Sillanpää, M.: Light absorption characteristics of carbonaceous aerosols in two remote stations of the southern fringe of the Tibetan Plateau, China, *Atmos. Environ.*, 143, 79-85, 10.1016/j.atmosenv.2016.08.042, 2016c.
- Li, C., Han, X., Kang, S., Yan, F., Chen, P., Hu, Z., Yang, J., Ciren, D., Gao, S., Sillanpää, M., Han, Y., Cui, Y., Liu, S., and Smith, K. R.: Heavy near-surface PM(2.5) pollution in Lhasa, China during a relatively static winter period, *Chemosphere*, 214, 314-318, 10.1016/j.chemosphere.2018.09.135, 2019.
- Li, C., Yan, F., Kang, S., Yan, C., Hu, Z., Chen, P., Gao, S., Zhang, C., He, C., Kaspari, S., and Stubbins, A.: Carbonaceous matter in the atmosphere and glaciers of the Himalayas and the Tibetan plateau: An investigative review, *Environ Int*, 146, 106281, 10.1016/j.envint.2020.106281, 2021a.
- Li, C., Zhang, C., Yan, F., Kang, S., Xu, Y., Liu, Y., Gao, Y., Chen, P., and He, C.: Importance of local non-fossil sources to carbonaceous aerosols at the eastern fringe of the Tibetan Plateau, China: Delta(14)C and delta(13)C evidences, *Environ Pollut*, 119858, 10.1016/j.envpol.2022.119858, 2022.
- Li, J., Wang, G., Wang, X., Cao, J., Sun, T., Cheng, C., Meng, J., Hu, T., and Liu, S.: Abundance, composition and source of atmospheric PM2.5 at a remote site in the Tibetan Plateau, China, *Tellus B: Chemical and Physical Meteorology*, 65, 20281, 10.3402/tellusb.v65i0.20281, 2013.
- Li, W. J., Chen, S. R., Xu, Y. S., Guo, X. C., Sun, Y. L., Yang, X. Y., Wang, Z. F., Zhao, X. D., Chen, J. M., and Wang, W. X.: Mixing state and sources of submicron regional background aerosols in the northern Qinghai-Tibet Plateau and the influence of biomass burning, *Atmos. Chem. Phys.*, 15, 13365-13376, 10.5194/acp-15-13365-2015, 2015.
- Li, Y., Yan, F., Kang, S., Zhang, C., Chen, P., Hu, Z., and Li, C.: Sources and light absorption characteristics of water-soluble organic carbon (WSOC) of atmospheric particles at a remote area in inner Himalayas and Tibetan Plateau, *Atmos. Res.*, 253, 105472, 10.1016/j.atmosres.2021.105472, 2021b.
- Lin, Y. C., Zhang, Y. L., Yu, M., Fan, M. Y., Xie, F., Zhang, W. Q., Wu, G., Cong, Z., and Michalski, G.: Formation Mechanisms and Source Apportionments of Airborne Nitrate Aerosols at a Himalayan-Tibetan Plateau Site: Insights from Nitrogen and Oxygen Isotopic Compositions, *Environ Sci Technol*, 55, 12261-12271, 10.1021/acs.est.1c03957, 2021.
- Liu, B., Cong, Z., Wang, Y., Xin, J., Wan, X., Pan, Y., Liu, Z., Wang, Y., Zhang, G., Wang, Z., Wang, Y., and Kang, S.: Background aerosol over the Himalayas and Tibetan Plateau: observed characteristics of aerosol mass loading, *Atmos. Chem. Phys.*, 17, 449-463, 10.5194/acp-17-449-2017, 2017.
- Liu, H., Wang, Q., Xing, L., Zhang, Y., Zhang, T., Ran, W., and Cao, J.: Measurement report: quantifying source contribution of fossil fuels and biomass-burning black carbon aerosol in the southeastern margin of the Tibetan Plateau, *Atmos. Chem. Phys.*, 21, 973-987, 10.5194/acp-21-973-2021, 2021.
- Ma, W. L., Qi, H., Baidron, S., Liu, L. Y., Yang, M., and Li, Y. F.: Implications for long-range atmospheric transport of polycyclic aromatic hydrocarbons in Lhasa, China, *Environmental science and pollution research international*, 20, 5525-5533, 10.1007/s11356-013-1577-1, 2013.
- Meng, J., Wang, G., Li, J., Cheng, C., and Cao, J.: Atmospheric oxalic acid and related secondary organic aerosols in Qinghai Lake, a continental background site in Tibet Plateau, *Atmos. Environ.*, 79, 582-589, 10.1016/j.atmosenv.2013.07.024, 2013.
- Meng, Y., Li, R., Zhao, Y., Cheng, H., Fu, H., Yan, Z., and Bing, H.: Chemical characterization and sources of PM2.5 at a high-alpine ecosystem in the Southeast Tibetan Plateau, China, *Atmos. Environ.*, 235, 117645, 10.1016/j.atmosenv.2020.117645, 2020.
- Middlebrook, A. M., Bahreini, R., Jimenez, J. L., and Canagaratna, M. R.: Evaluation of Composition-

- Dependent Collection Efficiencies for the Aerodyne Aerosol Mass Spectrometer using Field Data, *Aerosol Sci. Technol.*, 46, 258-271, 10.1080/02786826.2011.620041, 2012.
- Ni, H., Yao, P., Zhu, C., Qu, Y., Tian, J., Ma, Y., Yang, L., Zhong, H., Huang, R. J., and Dusek, U.: Non-Fossil Origin Explains the Large Seasonal Variation of Highly Processed Organic Aerosol in the Northeastern Tibetan Plateau (3,200 m a.s.l.), *Geophys. Res. Lett.*, 50, 10.1029/2023gl104710, 2023.
- Niu, H., Kang, S., Wang, H., Zhang, R., Lu, X., Qian, Y., Wang, S., Paudyal, R., Shi, X., and Yan, X.: Spatio-temporal variability and light absorption property of carbonaceous aerosol in a typical glacierization region of the Tibetan Plateau, *Atmospheric Chemistry and Physics Discussions*, 1-43, 10.5194/acp-2017-865, 2017.
- Paatero, P., and Tapper, U.: Positive matrix factorization: A non-negative factor model with optimal utilization of error estimates of data values, *Environmetrics*, 5, 111-126, 10.1002/env.3170050203, 1994.
- Ran, L., Deng, Z., Wu, Y., Li, J., Bai, Z., Lu, Y., Zhuoga, D., and Bian, J.: Measurement report: Vertical profiling of particle size distributions over Lhasa, Tibet – tethered balloon-based in situ measurements and source apportionment, *Atmos. Chem. Phys.*, 22, 6217-6229, 10.5194/acp-22-6217-2022, 2022.
- Ricchiazzi, P., Yang, S., Gautier, C., and Sowle, D.: SBDART: A Research and Teaching Software Tool for Plane-Parallel Radiative Transfer in the Earth's Atmosphere, *Bull. Am. Meteorol. Soc.*, 79, 2101-2114, 10.1175/1520-0477(1998)079<2101:Sarats>2.0.Co;2, 1998.
- Roberts, G. C., and Nenes, A.: A Continuous-Flow Streamwise Thermal-Gradient CCN Chamber for Atmospheric Measurements, *Aerosol Science and Technology*, 39, 206-221, 10.1080/027868290913988, 2005.
- Schueneman, M. K., Nault, B. A., Campuzano-Jost, P., Jo, D. S., Day, D. A., Schroder, J. C., Palm, B. B., Hodzic, A., Dibb, J. E., and Jimenez, J. L.: Aerosol pH indicator and organosulfate detectability from aerosol mass spectrometry measurements, *Atmos. Meas. Tech.*, 14, 2237-2260, 10.5194/amt-14-2237-2021, 2021.
- Su, H.-J., Xin, J.-Y., Ma, Y.-J., Liu, Z., Wen, T.-X., Wang, S.-G., Fan, G.-Z., Li, W., Wang, L., He, Z.-M., and Wang, Y.-S.: Effects of transport on aerosols over the eastern slope of the Tibetan Plateau: synergistic contribution of Southeast Asia and the Sichuan Basin, *Atmospheric and Oceanic Science Letters*, 11, 425-431, 10.1080/16742834.2018.1512832, 2018.
- Tang, L., Hu, M., Shang, D., Fang, X., Mao, J., Xu, W., Zhou, J., Zhao, W., Wang, Y., Zhang, C., Zhang, Y., Hu, J., Zeng, L., Ye, C., Guo, S., and Wu, Z.: High frequency of new particle formation events driven by summer monsoon in the central Tibetan Plateau, China, 10.5194/acp-2022-440, 2022.
- Ulbrich, I. M., Canagaratna, M. R., Zhang, Q., Worsnop, D. R., and Jimenez, J. L.: Interpretation of organic components from Positive Matrix Factorization of aerosol mass spectrometric data, *Atmos. Chem. Phys.*, 9, 2891-2918, 10.5194/acp-9-2891-2009, 2009.
- Wan, X., Kang, S., Wang, Y., Xin, J., Liu, B., Guo, Y., Wen, T., Zhang, G., and Cong, Z.: Size distribution of carbonaceous aerosols at a high-altitude site on the central Tibetan Plateau (Nam Co Station, 4730m.a.s.l.), *Atmos. Res.*, 153, 155-164, 10.1016/j.atmosres.2014.08.008, 2015.
- Wan, X., Kang, S., Xin, J., Liu, B., Wen, T., Wang, P., Wang, Y., and Cong, Z.: Chemical composition of size-segregated aerosols in Lhasa city, Tibetan Plateau, *Atmos. Res.*, 174-175, 142-150, 10.1016/j.atmosres.2016.02.005, 2016.
- Wan, X., Fu, P., Kang, S., Kawamura, K., Wu, G., Li, Q., Gao, S., and Cong, Z.: Organic aerosols in the inland Tibetan Plateau: New insights from molecular tracers, *Science of the Total Environment*, 884, 163797, 10.1016/j.scitotenv.2023.163797, 2023.

- Wang, J., Zhang, Q., Chen, M., Collier, S., Zhou, S., Ge, X., Xu, J., Shi, J., Xie, C., Hu, J., Ge, S., Sun, Y., and Coe, H.: First Chemical Characterization of Refractory Black Carbon Aerosols and Associated Coatings over the Tibetan Plateau (4730 m a.s.l), *Environ. Sci. Technol.*, 51, 14072-14082, 10.1021/acs.est.7b03973, 2017.
- Wang, J., Cao, X., Li, M., Tang, C., Zhang, Z., Zhang, H., Tian, P., Liang, J., Zhang, L., and Shi, J.: Optical characteristics of aerosol and its potential sources over Nam Co in the Tibetan Plateau during Asian summer monsoon period, *Atmos. Environ.*, 298, 10.1016/j.atmosenv.2023.119611, 2023.
- Wang, Q., Cao, J., Han, Y., Tian, J., Zhu, C., Zhang, Y., Zhang, N., Shen, Z., Ni, H., Zhao, S., and Wu, J.: Sources and physicochemical characteristics of black carbon aerosol from the southeastern Tibetan Plateau: internal mixing enhances light absorption, *Atmos. Chem. Phys.*, 18, 4639-4656, 10.5194/acp-18-4639-2018, 2018.
- Wang, Q., Han, Y., Ye, J., Liu, S., Pongpiachan, S., Zhang, N., Han, Y., Tian, J., Wu, C., Long, X., Zhang, Q., Zhang, W., Zhao, Z., and Cao, J.: High Contribution of Secondary Brown Carbon to Aerosol Light Absorption in the Southeastern Margin of Tibetan Plateau, *Geophys. Res. Lett.*, 46, 4962-4970, 10.1029/2019gl082731, 2019a.
- Wang, Y., Hu, M., Lin, P., Tan, T., Li, M., Xu, N., Zheng, J., Du, Z., Qin, Y., Wu, Y., Lu, S., Song, Y., Wu, Z., Guo, S., Zeng, L., Huang, X., and He, L.: Enhancement in Particulate Organic Nitrogen and Light Absorption of Humic-Like Substances over Tibetan Plateau Due to Long-Range Transported Biomass Burning Emissions, *Environ. Sci. Technol.*, 53, 14222-14232, 10.1021/acs.est.9b06152, 2019b.
- Wei, N., Ma, C., Liu, J., Wang, G., Liu, W., Zhuoga, D., Xiao, D., and Yao, J.: Size-Segregated Characteristics of Carbonaceous Aerosols during the Monsoon and Non-Monsoon Seasons in Lhasa in the Tibetan Plateau, *Atmosphere*, 10, 10.3390/atmos10030157, 2019a.
- Wei, N., Xu, Z., Liu, J., Wang, G., Liu, W., Zhuoga, D., Xiao, D., and Yao, J.: Characteristics of size distributions and sources of water-soluble ions in Lhasa during monsoon and non-monsoon seasons, *J Environ Sci (China)*, 82, 155-168, 10.1016/j.jes.2019.02.017, 2019b.
- Wu, G., Wan, X., Gao, S., Fu, P., Yin, Y., Li, G., Zhang, G., Kang, S., Ram, K., and Cong, Z.: Humic-Like Substances (HULIS) in Aerosols of Central Tibetan Plateau (Nam Co, 4730 m asl): Abundance, Light Absorption Properties, and Sources, *Environ. Sci. Technol.*, 52, 7203-7211, 10.1021/acs.est.8b01251, 2018.
- Wu, G., Wan, X., Ram, K., Li, P., Liu, B., Yin, Y., Fu, P., Loewen, M., Gao, S., Kang, S., Kawamura, K., Wang, Y., and Cong, Z.: Light absorption, fluorescence properties and sources of brown carbon aerosols in the Southeast Tibetan Plateau, *Environ. Pollut.*, 257, 113616, 10.1016/j.envpol.2019.113616, 2020.
- Xin, J., Gong, C., Wang, S., and Wang, Y.: Aerosol direct radiative forcing in desert and semi-desert regions of northwestern China, *Atmos. Res.*, 171, 56-65, 10.1016/j.atmosres.2015.12.004, 2016.
- Xu, J., Wang, Z., Yu, G., Qin, X., Ren, J., and Qin, D.: Characteristics of water soluble ionic species in fine particles from a high altitude site on the northern boundary of Tibetan Plateau: Mixture of mineral dust and anthropogenic aerosol, *Atmos. Res.*, 143, 43-56, 10.1016/j.atmosres.2014.01.018, 2014.
- Xu, J., Zhang, Q., Wang, Z. B., Yu, G. M., Ge, X. L., and Qin, X.: Chemical composition and size distribution of summertime PM_{2.5} at a high altitude remote location in the northeast of the Qinghai-Xizang (Tibet) Plateau: insights into aerosol sources and processing in free troposphere, *Atmos. Chem. Phys.*, 15, 5069-5081, 10.5194/acp-15-5069-2015, 2015.
- Xu, J., Zhang, Q., Shi, J., Ge, X., Xie, C., Wang, J., Kang, S., Zhang, R., and Wang, Y.: Chemical characteristics of submicron particles at the central Tibetan Plateau: insights from aerosol mass

- spectrometry, *Atmos. Chem. Phys.*, 18, 427-443, 10.5194/acp-18-427-2018, 2018a.
- Xu, J., Hettiyadura, A. P. S., Liu, Y., Zhang, X., Kang, S., and Laskin, A.: Regional Differences of Chemical Composition and Optical Properties of Aerosols in the Tibetan Plateau, *J. Geophys. Res. Atmos.*, 125, 10.1029/2019jd031226, 2020.
- Xu, J., Hettiyadura, A. P. S., Liu, Y., Zhang, X., Kang, S., and Laskin, A.: Atmospheric Brown Carbon on the Tibetan Plateau: Regional Differences in Chemical Composition and Light Absorption Properties, *Environmental Science & Technology Letters*, 9, 219-225, 10.1021/acs.estlett.2c00016, 2022a.
- Xu, W., Bian, Y., Lin, W., Zhang, Y., Wang, Y., Ma, Z., Zhang, X., Zhang, G., Ye, C., and Xu, X.: O₃ and PAN in southern Tibetan Plateau determined by distinct physical and chemical processes, *Atmos. Chem. Phys.*, 23, 7635-7652, 10.5194/acp-23-7635-2023, 2023.
- Xu, X., Zhang, H., Lin, W., Wang, Y., Xu, W., and Jia, S.: First simultaneous measurements of peroxyacetyl nitrate (PAN) and ozone at Nam Co in the central Tibetan Plateau: impacts from the PBL evolution and transport processes, *Atmos. Chem. Phys.*, 18, 5199-5217, 10.5194/acp-18-5199-2018, 2018b.
- Xu, Y., Li, Q., Xie, S., Zhang, C., Yan, F., Liu, Y., Kang, S., Gao, S., and Li, C.: Composition and sources of heavy metals in aerosol at a remote site of Southeast Tibetan Plateau, China, *Science of the Total Environment*, 845, 157308, 10.1016/j.scitotenv.2022.157308, 2022b.
- Yang, Y., Zhou, R., Yan, Y., Yu, Y., Liu, J., Di, Y., Du, Z., and Wu, D.: Seasonal variations and size distributions of water-soluble ions of atmospheric particulate matter at Shigatse, Tibetan Plateau, *Chemosphere*, 145, 560-567, 10.1016/j.chemosphere.2015.11.065, 2016.
- Yuan, Q., Xu, J., Wang, Y., Zhang, X., Pang, Y., Liu, L., Bi, L., Kang, S., and Li, W.: Mixing State and Fractal Dimension of Soot Particles at a Remote Site in the Southeastern Tibetan Plateau, *Environ. Sci. Technol.*, 53, 8227-8234, 10.1021/acs.est.9b01917, 2019.
- Zhang, L., Tang, C., Huang, J., Du, T., Guan, X., Tian, P., Shi, J., Cao, X., Huang, Z., Guo, Q., Zhang, H., Wang, M., Zeng, H., Wang, F., and Dolkar, P.: Unexpected High Absorption of Atmospheric Aerosols Over a Western Tibetan Plateau Site in Summer, *J. Geophys. Res. Atmos.*, 126, 10.1029/2020jd033286, 2021a.
- Zhang, N., Cao, J., Liu, S., Zhao, Z., Xu, H., and Xiao, S.: Chemical composition and sources of PM_{2.5} and TSP collected at Qinghai Lake during summertime, *Atmos. Res.*, 138, 213-222, 10.1016/j.atmosres.2013.11.016, 2014.
- Zhang, N., Cao, J., Huang, R., He, Y., Wang, Q., and Zhu, C.: Seasonal Variation, Sources and Transport of Aerosols at Lijiang, Southeast Tibetan Plateau, *Aerosol Air Qual. Res.*, 16, 1579-1590, 10.4209/aaqr.2015.07.0470, 2016.
- Zhang, Q., Jimenez, J. L., Worsnop, D., and Canagaratna, M.: A case study of urban particle acidity and its influence on secondary organic aerosol, *Environ. Sci. Technol.*, 41, 3213-3219, 10.1021/es061812j, 2007.
- Zhang, Q., Jimenez, J. L., Canagaratna, M. R., Ulbrich, I. M., Ng, N. L., Worsnop, D. R., and Sun, Y.: Understanding atmospheric organic aerosols via factor analysis of aerosol mass spectrometry: a review, *Anal. Bioanal. Chem.*, 401, 3045-3067, 10.1007/s00216-011-5355-y, 2011.
- Zhang, X., Xu, J., Kang, S., Liu, Y., and Zhang, Q.: Chemical characterization of long-range transport biomass burning emissions to the Himalayas: insights from high-resolution aerosol mass spectrometry, *Atmos. Chem. Phys.*, 18, 4617-4638, 10.5194/acp-18-4617-2018, 2018.
- Zhang, X., Xu, J., Kang, S., Zhang, Q., and Sun, J.: Chemical characterization and sources of submicron

- aerosols in the northeastern Qinghai–Tibet Plateau: insights from high-resolution mass spectrometry, *Atmos. Chem. Phys.*, 19, 7897-7911, 10.5194/acp-19-7897-2019, 2019.
- Zhang, X., Xu, J., and Kang, S.: Chemical characterization of submicron particulate matter (PM₁) emitted by burning highland barley in the northeastern part of the Qinghai–Tibet Plateau, *Atmos. Environ.*, 224, 117351, 10.1016/j.atmosenv.2020.117351, 2020.
- Zhang, X., Xu, J., Kang, S., Sun, J., Shi, J., Gong, C., Sun, X., Du, H., Ge, X., and Zhang, Q.: Regional Differences in the Light Absorption Properties of Fine Particulate Matter Over the Tibetan Plateau: Insights From HR-ToF-AMS and Aethalometer Measurements, *J. Geophys. Res. Atmos.*, 126, 10.1029/2021jd035562, 2021b.
- Zhang, Y., Xu, J., Shi, J., Xie, C., Ge, X., Wang, J., Kang, S., and Zhang, Q.: Light absorption by water-soluble organic carbon in atmospheric fine particles in the central Tibetan Plateau, *Environ. Sci. Pollut. Res.*, 24, 21386-21397, 10.1007/s11356-017-9688-8, 2017.
- Zhao, S., Ming, J., Xiao, C., Sun, W., and Qin, X.: A preliminary study on measurements of black carbon in the atmosphere of northwest Qilian Shan, *J. Environ. Sci.*, 24, 152-159, 10.1016/s1001-0742(11)60739-0, 2012.
- Zhao, S., Ming, J., Sun, J., and Xiao, C.: Observation of carbonaceous aerosols during 2006-2009 in Nyainqentanglha Mountains and the implications for glaciers, *Environmental science and pollution research international*, 20, 5827-5838, 10.1007/s11356-013-1548-6, 2013a.
- Zhao, S., Qi, S., Yu, Y., Kang, S., Dong, L., Chen, J., and Yin, D.: Measurement report: Contrasting elevation-dependent light absorption by black and brown carbon: lessons from in situ measurements from the highly polluted Sichuan Basin to the pristine Tibetan Plateau, *Atmos. Chem. Phys.*, 22, 14693-14708, 10.5194/acp-22-14693-2022, 2022a.
- Zhao, W., Zhang, X., Zhai, L., Shen, X., and Xu, J.: Chemical characterization and sources of submicron aerosols in Lhasa on the Qinghai–Tibet Plateau: Insights from high-resolution mass spectrometry, *Sci. Total Environ.*, 815, 10.1016/j.scitotenv.2021.152866, 2022b.
- Zhao, Z., Cao, J., Shen, Z., Xu, B., Zhu, C., Chen, L.-W. A., Su, X., Liu, S., Han, Y., Wang, G., and Ho, K.: Aerosol particles at a high-altitude site on the Southeast Tibetan Plateau, China: Implications for pollution transport from South Asia, *J. Geophys. Res. Atmos.*, 118, 11360-11375, 10.1002/jgrd.50599, 2013b.
- Zhao, Z., Cao, J., Chow, J. C., Watson, J. G., Chen, A. L. W., Wang, X., Wang, Q., Tian, J., Shen, Z., Zhu, C., Liu, S., Tao, J., Ye, Z., Zhang, T., Zhou, J., and Tian, R.: Multi-wavelength light absorption of black and brown carbon at a high-altitude site on the Southeastern margin of the Tibetan Plateau, China, *Atmos. Environ.*, 212, 54-64, 10.1016/j.atmosenv.2019.05.035, 2019a.
- Zhao, Z., Wang, Q., Li, L., Han, Y., Ye, Z., Pongpiachan, S., Zhang, Y., Liu, S., Tian, R., and Cao, J.: Characteristics of PM_{2.5} at a High-Altitude Remote Site in the Southeastern Margin of the Tibetan Plateau in Premonsoon Season, *Atmosphere*, 10, 645, 10.3390/atmos10110645, 2019b.
- Zheng, J., Hu, M., Du, Z., Shang, D., Gong, Z., Qin, Y., Fang, J., Gu, F., Li, M., Peng, J., Li, J., Zhang, Y., Huang, X., He, L., Wu, Y., and Guo, S.: Influence of biomass burning from South Asia at a high-altitude mountain receptor site in China, *Atmos. Chem. Phys.*, 17, 6853-6864, 10.5194/acp-17-6853-2017, 2017.
- Zhou, J., Tie, X., Xu, B., Zhao, S., Wang, M., Li, G., Yang, S., Chang, L., and Cao, J.: Black carbon (BC) in North Tibetan Mountain; Effect of Kuwait fires on glacier, *Atmospheric Chemistry and Physics Discussions*, 1-24, 10.5194/acp-2018-448, 2018.
- Zhu, C.-S., Qu, Y., Dai, W.-T., Zhang, N.-N., Zhang, Z.-S., and Cao, J.-J.: Nonnegligible biogenic organic

- aerosol and the correlations with light absorption at three high altitude locations in the Qinghai-Tibetan Plateau, *Atmos. Environ.*, 291, 10.1016/j.atmosenv.2022.119394, 2022.
- Zhu, C. S., Cao, J. J., Hu, T. F., Shen, Z. X., Tie, X. X., Huang, H., Wang, Q. Y., Huang, R. J., Zhao, Z. Z., Mocnik, G., and Hansen, A. D. A.: Spectral dependence of aerosol light absorption at an urban and a remote site over the Tibetan Plateau, *Sci. Total Environ.*, 590-591, 14-21, 10.1016/j.scitotenv.2017.03.057, 2017.
- Zhu, C. S., Cao, J. J., Huang, R. J., Shen, Z. X., Wang, Q. Y., and Zhang, N. N.: Light absorption properties of brown carbon over the southeastern Tibetan Plateau, *Sci. Total Environ.*, 625, 246-251, 10.1016/j.scitotenv.2017.12.183, 2018.
- Zhu, C. S., Li, L. J., Huang, H., Dai, W. T., Lei, Y. L., Qu, Y., Huang, R. J., Wang, Q. Y., Shen, Z. X., and Cao, J. J.: n-Alkanes and PAHs in the Southeastern Tibetan Plateau: Characteristics and Correlations With Brown Carbon Light Absorption, *J. Geophys. Res. Atmos.*, 125, 10.1029/2020jd032666, 2020.
- Zhu, C. S., Qu, Y., Huang, H., Chen, J., Dai, W. T., Huang, R. J., and Cao, J. J.: Black Carbon and Secondary Brown Carbon, the Dominant Light Absorption and Direct Radiative Forcing Contributors of the Atmospheric Aerosols Over the Tibetan Plateau, *Geophys. Res. Lett.*, 48, 10.1029/2021gl092524, 2021.